



Journal of Advanced Research in Fluid Mechanics and Thermal Sciences

Journal homepage:
https://semarakilmu.com.my/journals/index.php/fluid_mechanics_thermal_sciences/index
ISSN: 2289-7879



The Effect of Palm Oil Biodiesel-Neat Diesel (B10-B50) Mixing Ratio on Physical Mechanism of Fuel Deposits Developed on Heated Al Surface

Favian Jikol¹, Mohd Zaid Akop^{1,*}, Yusmady Mohamed Arifin¹, Mohd Azli Salim¹, Safarudin Gazali Herawan²

¹ Faculty of Mechanical Technology and Engineering, Universiti Teknikal Malaysia Melaka, 76100 Durian Tunggal, Melaka, Malaysia

² Industrial Engineering Department, Faculty of Engineering, Bina Nusantara University, Indonesia

ARTICLE INFO

Article history:

Received 24 October 2023

Received in revised form 28 March 2024

Accepted 9 April 2024

Available online 30 April 2024

Keywords:

Biodiesel; blend ratio; deposit composition; SEM; wet/dry condition

ABSTRACT

To improve the physicochemical properties of biodiesel, researchers have been mixing pure biodiesel with neat diesel to produce blended fuels with certain blending ratios. However, one of the issues when combining ordinary diesel with biodiesel is the formation of deposits. In this study, the hot surface deposition test (HSDT) method was employed to investigate the effect of the mixing ratio on the deposition of diesel fuel (DF) and its blends with Malaysian palm oil biodiesel (B10-B50). The accumulated fuel deposits produced by the test fuels up to ND=16000 droplets were studied based on visual inspection and the use of a scanning electron microscope (SEM) to study the deposits' composition. Generally, the higher the blend ratio, the more deposits were formed on the hot plate. Furthermore, a greater mass of deposits was produced during the wet condition ($t_{imp}=3$ seconds) test compared to that of the dry condition ($t_{imp}=7$ seconds) test. Deposits' distribution area produced by the B30, B40, and B50 fuels were larger and appeared to be oily/greasy. Meanwhile, deposits produced by DF, B10, and B20 seem to be dry. The radius of the solid deposit was also larger during the wet condition test. For dry condition test at droplet ND=16000, the mass of deposit produced was 3.7mg (4mm radius) for DF, 3.9mg (5mm radius) for B10, 17.1mg (9mm radius) for B20, 24.0mg (9mm radius) for B30, 25.1mg (9mm radius) for B40, and 28.8mg (7mm radius) for B50. On the other hand, for the wet condition test, the mass of the deposit generated was 4.4mg (4mm radius) for DF, 8.9mg (7mm radius) for B10, 20.4mg (11mm radius) for B20, 31.1mg (13mm radius) for B30, 62.4mg (15mm radius) for B40, and 58.2mg (13mm radius) for B50, respectively. Additionally, the SEM analysis showed that the deposits' composition for each test fuel primarily consists of carbon (>65%), with relatively lower oxygen concentration (<35%). The dry and wet condition also has a significant impact on the various deposits' morphology.

1. Introduction

Palm oil biodiesel is the most utilized biodiesel in Malaysia [1-3]. Biodiesel, or known as mono-alkyl ester of long-chain fatty acids (FAME) is obtained from renewable lipids such as vegetable oils,

* Corresponding author.

E-mail address: zaid@utem.edu.my

<https://doi.org/10.37934/arfmts.116.2.112130>

animal fats, and alcohol [4]. It is environmentally friendly, renewable, non-toxic, non-flammable, and non-explosive. Its qualities are comparable to those of diesel fuel, where the main benefits of biodiesel are its ability to be blended with diesel fuel in any ratio, and able to be used in diesel engines without the need for modification [5-8]. Apart from that, alcohol, which is already readily available, can be blended with biodiesel and neat diesel fuel [9]. The fact that it is free of toxic compounds and emits fewer harmful emissions into the environment makes biodiesel a popular alternative to non-renewable fossil fuels. It is possible to enhance the percentage of renewable energy in the automotive sector and maybe increase the lifespan of internal combustion engines by employing a higher blend level of biodiesel [10]. However, the primary issue of pure biodiesel is the fuel's extremely high viscosity, which is 10–20 times more than that of regular diesel, hence, mixing with ordinary diesel or other components is preferable to cope with this issue [11]. Compared to pure diesel, biodiesel possesses higher carbon residues due to variations in chemical composition and molecular structure, which escalates the chance of carbon deposition inside the combustion chamber [12]. Additionally, as documented in our previous work, deposit formation inside the combustion chamber also affects the mechanical and emissions performance of the engine [13].

The use of biodiesel in a diesel engine can lead to complete combustion because of the presence of oxygen elements in the biodiesel molecule [14]. However, the composition of the deposits generated will vary as a result of the mixing of the fuels. This is because biodiesel will differ from diesel fuel in terms of deposit production due to its higher oxygen concentration [15]. Apart from that, the negative side of adding more biodiesel into neat diesel is that biodiesel has poor injection properties. Uyumaz *et al.*, [14] explained that the size of the biodiesel droplets that were injected also grew as the proportion of biodiesel in the fuel mixtures rose. As a result, fuel consumption rises and biodiesel atomization degrades. This is in agreement with Sase *et al.*, [16] who stated that biodiesel has significantly larger mean droplet sizes than diesel fuel because of biodiesel's high viscosity and low volatility, hence, making it difficult to atomize the fuel and combine it with air.

Unburned hydrocarbons and carbon monoxide are produced by the incomplete combustion of the heterogeneous mixture. Additionally, carbon deposits are formed in or on the cylinder wall and head, valve, piston, and injectors within the combustion chamber [17]. Fuel oxidation and soot production during engine combustion are linked to carbon deposits [18]. Modern diesel fuel systems have higher operating pressures and temperatures, which can accelerate the oxidation and breakdown of the chemically unstable components of diesel fuels, especially those found in FAME, and increase the likelihood of internal diesel injector deposits forming [19]. Zhang *et al.*, [20] stated that in internal combustion engines (ICE), the existence of combustion chamber deposits (CCD) is unavoidable. This is in agreement with Cheng [21], who explained that the CCD has existed since the inception of ICE. The deposit formation inside the combustion chamber is an undesired but unavoidable by-product of engine combustion. The author also mentioned that the shape of the deposits generated in various regions of the combustion chamber varied greatly, and the variations in surface temperature were the primary cause of the discrepancies. Moreover, when deposits form, they are typically thick and gummy. Once they settle in an engine, they frequently harden, which can lead to the development of a blockage location [22].

Even though combustion chamber deposits consist of complex materials that are hard to characterize as studied by Husnawan *et al.*, [23], the study of the physical mechanism or morphology of the deposit is important as it is one of the factors that could influence the severity of deposit development on the diesel engine parts such as the injector which being studied by Rounthwaite *et al.*, [24]. However, there was no biodiesel involved in the author's experimental work. Another author, Cavalheiro *et al.*, [25] mentioned that the presence of solid residues in biodiesel combined with diesel can lead to issues with the fuel filters, nozzles, ignition, and loss of engine performance.

In addition, Elsanusi *et al.*, [26] in his study cited that the high viscosity of biodiesel resulted in engine operational issues such as incomplete combustion and deposit formation. Furthermore, various types of aberrant combustion might result from deposit accumulation. It is evident in one form how negatively it affects engine performance. For instance, deposited hot patches that ignite uncontrollably and cause knocking, run-on, and rumble.

Engine emissions are also impacted by irregular combustion brought on by deposits in addition to degraded engine performance. Pham [27] also pointed out that many engine parameters will be negatively impacted by deposits on different engine components, including air residue, airflow, compression ratio, spray characteristics, knock, thermal conductivity, and catalyst activity. In another study by Feld and Oberender [28], they pointed out that even small concentrations of deposits can result in serious concerns, including poor filterability, filter obstruction, corrosion, and technical problems like declining injection precision, flow behavior, and spray accuracy. It is essential to note that droplets in spray combustion differ from single ones. In general, biodiesel has poor spray characteristics owing to its high density, viscosity, and surface tension. Bhikuning *et al.*, [29] stated that biodiesels are hard to vaporize due to their high density, viscosity, and surface tension. These three properties of biodiesel are the reason for the formation of larger droplets which are more difficult to vaporize and consequently lead to poor spray characteristics. Furthermore, the evaporation and combustion processes of these droplets are influenced by the presence of other droplets in their surroundings [30]. As stated by Hoang and Le [31] atomization level of fuel is evaluated by the spray characteristics and the changes for these spray parameters were mainly constituted by the formation of the deposit inside the injector hole. The formed deposits are the results of incomplete combustion of fuel which is commonly associated with biodiesel due to their larger droplets that are harder to vaporize.

The different mixing ratios between biodiesel and neat diesel fuel will produce different physicochemical properties of the blends, which could influence the deposition characteristics of the tested fuel when impinged on the surface of a heated aluminum alloy plate. The physicochemical properties of fuel that were frequently discussed in the literature were the density, kinematic viscosity, heating value, flash point, cetane number, cloud point, and pour point [32,33]. The amount of generated deposit is dependent upon the fuel type and different parts of the combustion chamber may experience different deposit growth mechanisms as a result of the fuel's physical characteristics [34,35], in this study the tested fuels were differentiated according to certain blend ratios. In general, when the biodiesel ratio in the fuel mixture is increased, the density and kinematic viscosity also increase. The atomization of biodiesel fuel mixes was negatively impacted by biodiesel's increased density and viscosity. This could lead to imperfect combustion, which eventually causes an increase in carbon deposits [36]. As a result, fuel cannot be atomized and evaporated adequately, which probably influences the physical appearance of the formed deposits, as more fuel residues are left unburned [14]. Different ratios of FAME in a fuel mixture will contribute to different deposit formation mechanisms, as reported by Birgel *et al.*, [37] who found out that B30 and B100 fuel accelerated the deposit formation compared to that of ordinary diesel fuel. Furthermore, Liaquat *et al.*, [38] in his study also compared the deposit's physical mechanism. The author found out that oily/greasy deposits were seen on injectors running DF, while dry deposits were seen on nozzles running the PB20 blend. This indicates that the FAME in a fuel influences the physical appearance of the generated deposits. Apart from that, researchers discovered that the substance of carbon deposits was often amorphous, porous, and distinguished by a heterogeneous granular structure in several investigations that classified deposit structures [39-41].

Deposits were likely created by the thermal disintegration of methyl ester molecules or the thermal decomposition of glycerine molecules that were present as impurities in the methyl ester,

as explained by Barker *et al.*, [42]. Because of the variations in surface temperatures and the processes that take place near these surfaces, deposits in various engine components have a wide range in nature and how they form [43]. Additionally, deposit formation is highly influenced by the temperature to which the fuel is exposed [44]. The temperature at which a deposit forms has a significant impact on the deposit's characteristics, where the deposit structure changes when the temperature changes [45]. However, in this work, the surface temperature of the hot plate was made constant to investigate thoroughly the effect of the blend ratio itself on the deposition mechanism.

In this study, the deposits from each test fuel were formed on the hot plate. The focus was to observe and distinguish the physical appearance of the formed deposits, given the test fuels' different mixing ratios. Compared to an actual engine bench test, the simplicity of this experimental method significantly overcame the longer test period and eventually reduced the operating cost. The results will be compared to that of diesel fuel to identify the impacts of increasing the ratio in palm oil biodiesel-diesel fuel mixture. Furthermore, the outcomes of this work can be used as a reference to simulate the severity of deposit formation inside the combustion chamber when a high blended palm oil biodiesel is used as a fuel. Thus, the development, composition, structure, and influencing elements of the deposit must therefore be studied to establish a foundation for mitigating engine deposits.

2. Methodology

The neat diesel fuel (DF) and the palm oil biodiesel-diesel fuel blend (B10-B50) used in this experiment were supplied by a local factory here in Malaysia. For the B10 fuel, a mixture of 10% palm oil biodiesel and 90% plain diesel was used as the biodiesel-diesel blend. The additional fuel mixtures, known as B20, B30, B40, and B50, were made by mixing palm oil biodiesel in neat diesel fuel in volume proportions of 20%, 30%, 40%, and 50%, respectively. As can be seen in Table 1, the trend was that the higher the blend ratio, the higher the density and kinematic viscosity of the fuel. Even though different ratios of fuel blends were used, the calculated diameter for the single fuel droplet was 2.3mm for the B10 fuel, and 2.2mm for DF, B20, B30, B40, and B50, respectively. Since the difference in droplet size was small, the droplets' size can be considered identical. Hence, for these test fuels, a higher blending ratio does not lead to a significant difference in the droplet size.

Table 1
Physicochemical properties of diesel fuel and blended Malaysian palm oil biodiesel (test limit: ASTM D7467) [33]

Properties	Fuel					
	DF	B10	B20	B30	B40	B50
Density (kg/m ³)	847	850	853	857	860	863
Kinematic viscosity (mm ² /s)	3.8	3.86	3.91	3.95	3.97	4.00
Heating value (MJ/kg)	45.21	44.23	44.12	43.13	42.95	42.74
Acid value (mg KOH/g)	0.16	0.18	0.22	0.26	0.30	0.33

Due to different engine sizes, technologies, and testing settings, the analysis of carbon deposits in diesel engines is complicated [35]. Thus, a simple method called the hot surface deposition test (HSDT) method was applied in this work as illustrated in Figure 1. This experimental concept to study the fuel deposition on a heated plate was implemented in the previous works [45-48]. The droplet was impinged on the center part of the plate as it is the hottest area as found out in our previous studies [49,50]. For the deposition test parameter, the test condition consisted of two conditions, which were identified as dry and wet conditions. The main difference between dry and wet

conditions is the droplet interval, which is related to the evaporation time of a fuel droplet. When the fuel has not entirely evaporated and the subsequent droplet has dropped back onto the hot plate, depositing deposits happen. This circumstance is also known as an overlap circumstance. The area of the deposit and the mass of the ensuing deposit are also influenced by the evaporation time [51]. For dry conditions, the impingement interval, t_{imp} , was set longer ($t_{imp}=7$ seconds) than the droplet lifetime of the test fuels, and vice versa for wet conditions ($t_{imp}=3$ seconds). This is to simulate the existence of wet conditions in the real combustion chamber. In terms of temperature, the surface temperature of the hot plate, T_s , was set to $T_s=315^\circ\text{C}$ for DF and $T_s=340^\circ\text{C}$ for the blended fuels B10-B50. These temperatures were set based on the maximum evaporation point (MEP) temperature for each fuel obtained from a separate fuel droplet evaporation characteristics test. Furthermore, the deposition test for each fuel was conducted until the droplet number $N_D=16000$ droplet for both dry and wet condition tests. After each set of experiments was completed, a photograph of the formed deposits was taken by using a Mirrorless Camera Sony A7III Model ILCE-7M3. To ensure the quality and consistency of the images taken, the camera setting (Focal length: 50mm, Aperture: f/2, Exposure time: 1/200, ISO speed: 200) and positioning (distance from lens to hot plate surface: 55cm) were fixed throughout the experiments. In this study, the physical appearance of deposits produced was observed and images were taken at droplet $N_D=4000$, $N_D=8000$, and $N_D=16000$. Furthermore, the radius of the solid deposit generated was also measured to correlate with the biodiesel mixing ratio and mass of the deposit produced. In addition, to identify the deposit's composition, a scanning electron microscope (SEM) was used. For the SEM, the images were taken at 500x magnification.

One of the factors that could affect the temperature measured by the thermocouple was its thermal contact resistance with the heated plate. However, the difference between the set temperature and the temperature measured by the thermocouple did not exceed $\pm 5^\circ\text{C}$. For droplet intervals, droplets might exit the injector needle at a shorter or longer time than the previous droplet. Hence, the tolerance for impingement interval was set to ± 1 second. Additionally, the droplet control valve was monitored and adjusted for every 1000 droplets to make sure the impingement interval for both wet and dry conditions was still within the ± 1 second tolerance.

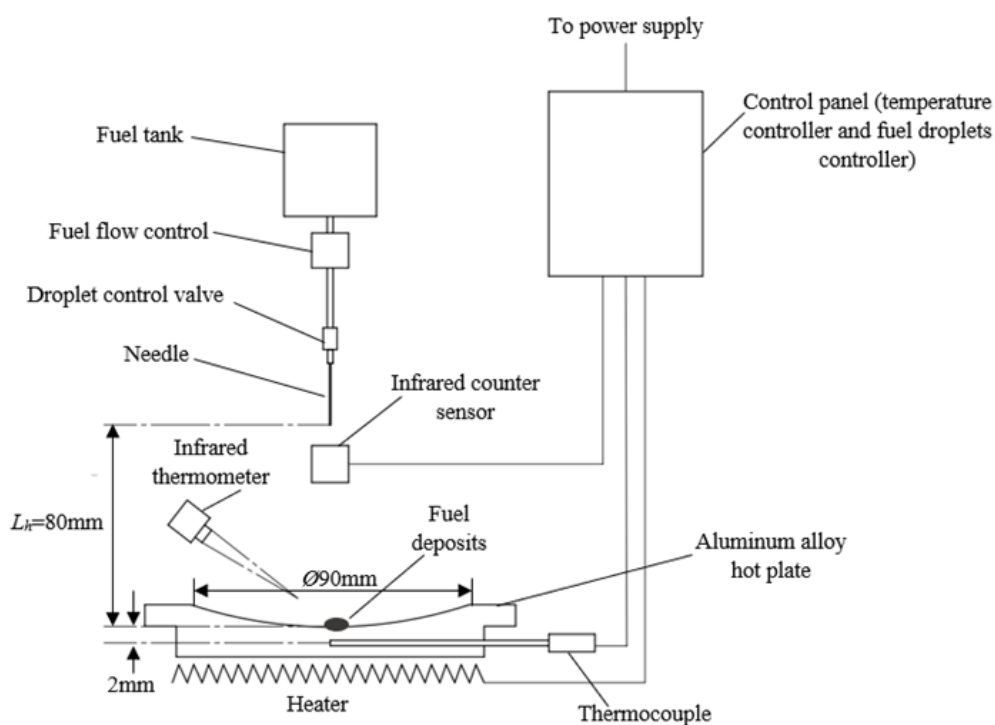


Fig. 1. Schematic diagram of HSDT setup

3. Results and Discussions

Photographs of accumulated deposits were captured at every $N_D=1000$ droplet repetition until reaching $N_D=16000$. In this study, these deposit images are crucial for observing and comparing the mechanisms of deposit formation for different fuels at varying impingement intervals of $t_{imp}=3$ seconds (simulating wet conditions) and $t_{imp}=7$ seconds (representing dry conditions). Furthermore, the deposit structures formed by the test fuels as the fuel droplet repetition increases play a key role in understanding deposit development behavior [40]. These structures also impact the heat transfer and thermal conductivity of the deposits.

Table 2 provides a comparison of deposit images on the hot plate surface at different stages of the deposition test: $N_D=4000$, $N_D=8000$ (mid-stage), and $N_D=16000$ (completion) for an impingement interval of $t_{imp}=7$ seconds, representing dry conditions. In this case, the impingement interval exceeds the droplet evaporation lifetime for each test fuel. Consequently, DF generated deposits at $N_D=4000$, $N_D=8000$, and $N_D=16000$ that displayed no apparent signs of deposit splashing, even at a lower hot plate surface temperature of $T_S=315^\circ\text{C}$. Unlike palm oil biodiesel fuels, DF contains fewer impurities but has a higher carbon residue content. Additionally, the absence of fuel components like glycerides contributes to fewer and thinner accumulated deposits for DF. The absence of glyceride components in DF, along with its lower carbon residue and impurity levels compared to biodiesel, suggests that any traces of deposit splashing were likely caused by the wet conditions themselves [52]. DF also produced the lowest amount of deposits compared to other fuels, with 0.4mg, 1.1mg, and 3.7mg at $N_D=4000$, $N_D=8000$, and $N_D=16000$, respectively, in the dry condition test.

For B10 fuel, the cumulative deposits at droplet $N_D=4000$, $N_D=8000$, and $N_D=16000$ were 1.2mg, 2.0mg, and 3.9mg, respectively. Despite the hot plate surface being hotter ($T_S=340^\circ\text{C}$) compared to DF, noticeable traces of deposit splashing were observed at all stages of the deposition test. However, the deposit splashing became less pronounced at $N_D=8000$ and decreased further at $N_D=16000$, possibly due to fuel deposit oxidation during the test. Nevertheless, the radius of solid deposits increased from droplet $N_D=4000$ to $N_D=16000$. The structure of the deposits formed at both droplet intervals was also denser and more porous. This can be attributed to the lower biodiesel content in B10 fuel, which led to faster evaporation and a drier deposit structure.

For B20 fuel, the deposit masses were 2.4mg ($N_D=4000$), 6.4mg ($N_D=8000$), and 17.1mg ($N_D=16000$). There were also significant differences in deposit splashes produced by B20 fuel compared to that of DF and B10 fuel. Moreover, there were noticeable changes in the deposit thickness. As the hot plate surface temperature and droplet interval were identical to the test on B10 fuel, it can be deduced that B20 deposition was greatly influenced by its biodiesel content.

In the case of B30 fuel, there were more pronounced differences in deposit distribution compared to B10 and B20 fuels, especially during the wet condition test. In the dry condition test, B30 fuel produced deposit masses of 3.9mg ($N_D=4000$), 9.3mg ($N_D=8000$), and 24.0mg ($N_D=16000$). Visual inspection of the B30 deposits revealed that their radius grew larger, leaving more unburned fuels on the hot plate surface. While some parts of the deposit surface appeared wetter and smoother, the majority remained rough and porous. These significant changes in the deposit's physical characteristics were likely influenced by the surface temperature of the accumulating deposits themselves. As more fuel droplets impinged on the hot plate, layers of deposits formed, becoming thicker and impacting the surface temperature of the deposits, consequently affecting their shape [34].

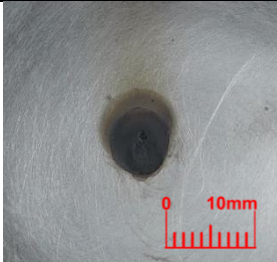
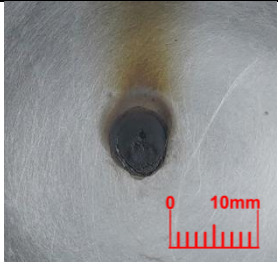
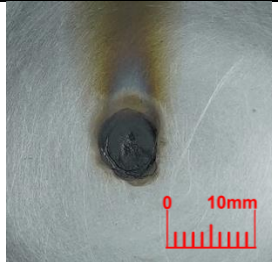
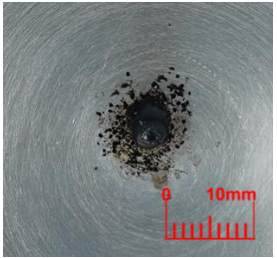
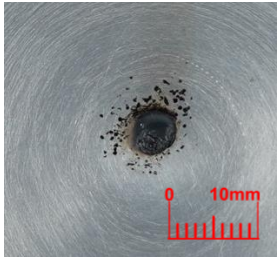


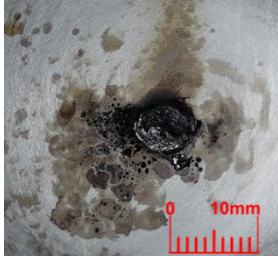
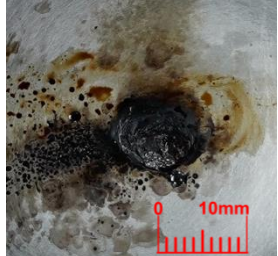
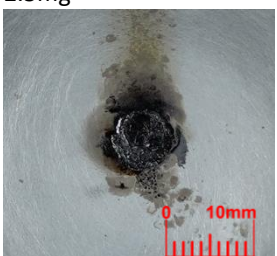

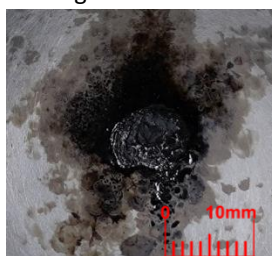
Photographic views of the deposits accumulated on the hot plate showed a similar deposit distribution for B40 fuel during the dry condition test when compared to B30 fuel. In addition, the

masses of generated deposits by B40 fuel (5.6mg ($N_D=4000$), 10.3mg ($N_D=8000$), and 25.1mg ($N_D=16000$)) were almost identical to B30 fuel.

For B50 fuels, more visible traces of deposit splashing were observed at $N_D=4000$, $N_D=8000$, and $N_D=16000$. The wider area covered by splash deposits for B50 fuel also resulted in a dirtier hot plate surface compared to other test fuels. In terms of deposit masses, B50 fuel exceeds other test fuels except for droplet $N_D=4000$, where B50 generated fewer deposits (4.7mg) compared to that of B40 fuel (5.6mg). This indicates that at the early stage of the test, B40 fuel deposition was more affected by the existence of wet conditions due to the increasing number of droplets. Nevertheless, B50 fuel produced the most deposits at droplet $N_D=8000$ (13.8mg) and $N_D=16000$ (28.8mg).

Table 2

Photograph of deposit at $N_D=4000$, $N_D=8000$, and $N_D=16000$ for dry condition

Fuel	Condition	Droplet number, N_D		
		$N_D=4000$	$N_D=8000$	$N_D=16000$
DF	$t_{imp}=7s$ $T_s=315^\circ C$	 0.4mg	 1.1mg	 3.7mg
B10	$t_{imp}=7s$ $T_s=340^\circ C$	 1.2mg	 2.0mg	 3.9mg
B20		 2.5mg	 6.4mg	 17.1mg
B30		 3.9mg	 9.3mg	 24.0mg

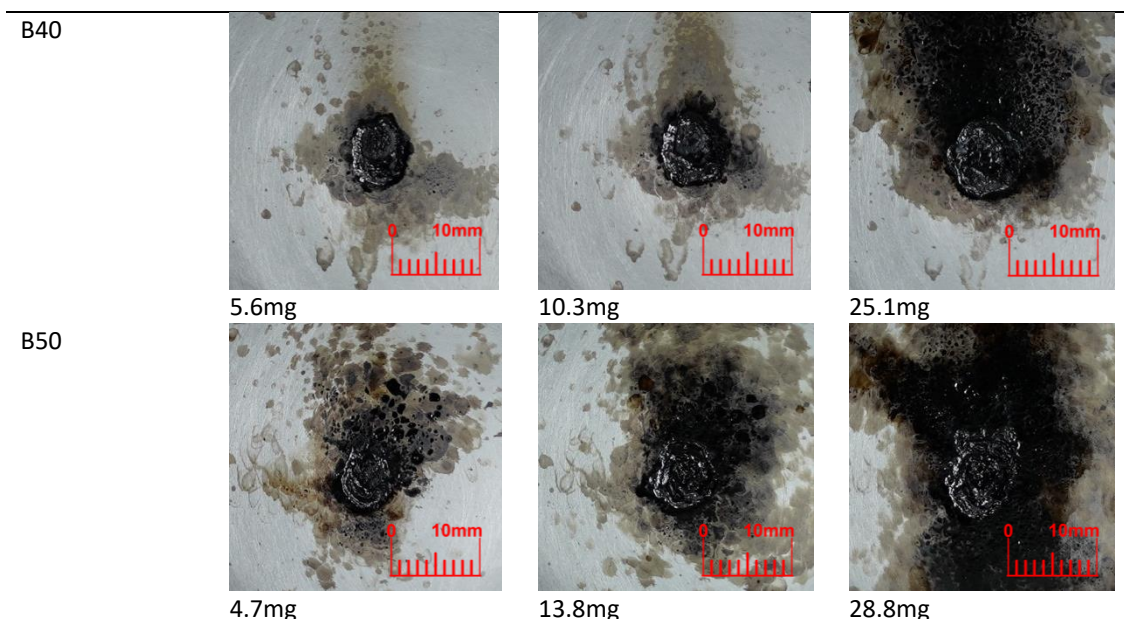


Table 3 displays the outcomes of deposition tests under wet conditions at $N_D=4000$, $N_D=8000$, and $N_D=16000$ for wet condition tests. In particular, significant disparities emerged in the deposit structures formed on the hot plate surface when the impingement interval was reduced to $t_{imp}=3$ seconds. The accumulated deposits for DF (0.6mg ($N_D=4000$), 1.9mg ($N_D=8000$), and 4.4mg ($N_D=16000$)) closely resembled those generated by DF during the dry condition test at $t_{imp}=7$ seconds. However, with an impingement interval of $t_{imp}=3$ seconds, there were observable traces of splash deposits created by DF. This phenomenon primarily arose due to the wet condition persisting on the surface of the resulting deposit when the impingement interval was set below DF's droplet evaporation lifetime.

Among the blends of palm oil biodiesel and diesel fuel, B10 stands out with the lowest density and kinematic viscosity. This characteristic likely contributes to B10 forming the least conspicuous deposit splashes and a smaller overall deposit distribution area compared to the other biodiesel blends. Furthermore, B10 also generated the least amount of deposits ((0.5mg ($N_D=4000$), 2.9mg ($N_D=8000$), and 8.9mg ($N_D=16000$)) when compared with B20-B50 fuel. In the case of blended biodiesel fuels ranging from B10 to B50, the deposits tend to be thicker and exhibit larger traces of deposit splash radius as the droplet number increases from $N_D=4000$ to $N_D=8000$, eventually reaching $N_D=16000$. This behavior is primarily attributed to the lower thermal conductivity of these deposits, causing their surface temperature to drop below that of the heated surface [48,53].

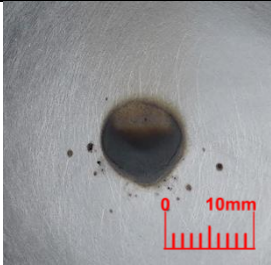
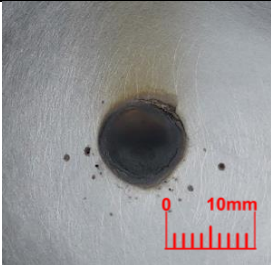
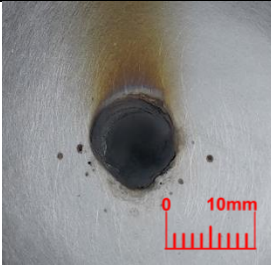
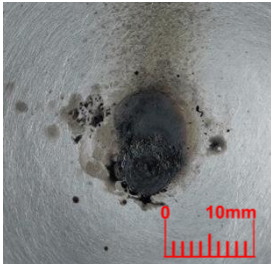
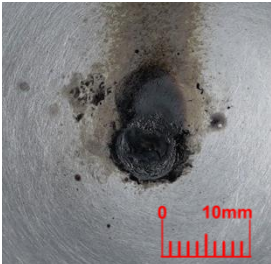
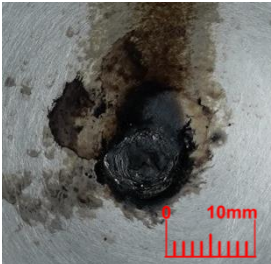
For B20 fuel, the amount of deposits formed on the hot plate exceeded that of B10. Specifically, B20 produced 5.1mg ($N_D=4000$), 10.1mg ($N_D=8000$), and 20.4mg ($N_D=16000$) of deposits. Interestingly, these deposits were notably rougher, particularly in the dry condition test, where the hot plate's surface appeared dirtier than in the dry condition test for B10 fuel. A similar finding was reported by Liaquat *et al.*, [54], who observed that injectors running on a 20% palm oil biodiesel-diesel fuel blend were dirtier than those running on pure diesel fuel.

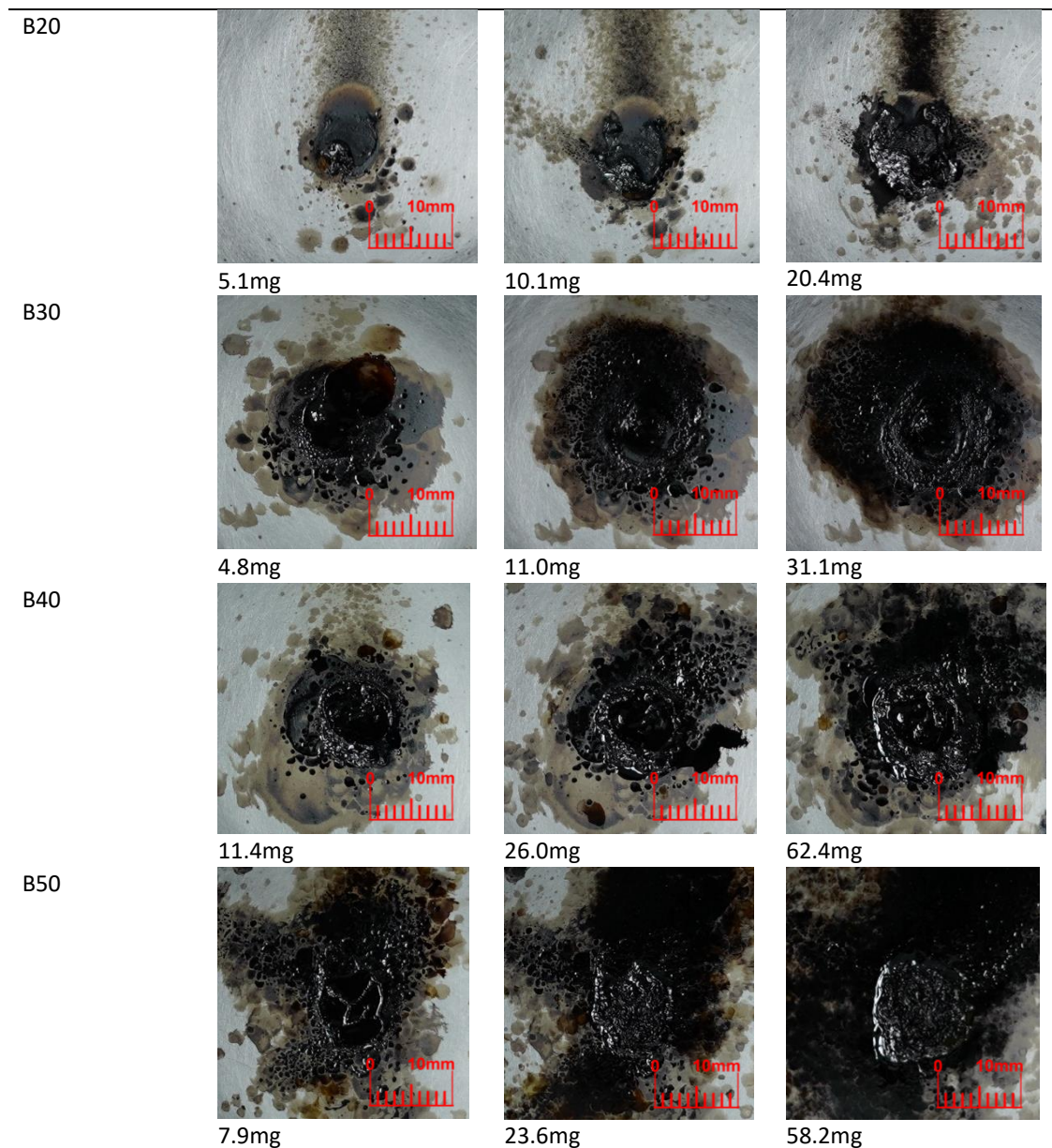
The deposits generated by B10-B50 fuels appeared as mound-like deposits with compact and porous structures. More liquid fuel stains were also present around the deposition area, especially for B30, B40, and B50 fuels. For B30 fuel, the masses of produced deposits were 4.8mg ($N_D=4000$), 11.0mg ($N_D=8000$), and 31.1mg ($N_D=16000$). The radius of solid deposits produced on the hot plate also increased significantly, particularly for B10-B50 fuels, compared to the dry condition test with a longer impingement interval of $t_{imp}=7$ seconds.

For B40 fuel, the masses of deposits generated on the hot plate were the highest compared to other test fuels (11.4mg ($N_D=4000$), 26.0mg ($N_D=8000$), and 62.4mg ($N_D=16000$)). The composition of the fuel significantly influences the amount of deposits on the hot plate. Specifically, B50 fuel, with a higher palm oil biodiesel blend, results in thicker deposits that spread over a larger area [52]. It is noteworthy that the deposits generated by B40 fuel, totalling 62.4mg at droplet $N_D=16000$, were the heaviest among all tested fuels in the wet condition test, followed by B50 fuel (7.9mg ($N_D=4000$), 23.6mg ($N_D=8000$), and 58.2mg ($N_D=16000$)). These findings contrast with most previous studies that suggested fuels with higher biodiesel content tend to produce more deposits. However, in terms of physical appearance, the deposit distribution of B50 fuel was the most extensive. The surface of the hot plate also appeared dirtier for both dry and wet conditions in the B50 fuel deposition test. Furthermore, the resulting deposits were thicker and appeared oily and greasy, indicating that more fuel residues did not evaporate on the hot plate. Similar findings were reported by Suryantoro *et al.*, [55], who described deposits produced by B50 fuel as moist and oily. The author also noted that the wetness of B50 deposits could be attributed to the presence of numerous fuel residues, making them flammable.

In actual engines, the surface temperature of deposits can vary depending on factors like engine specifications, load, speed, and environmental conditions. Thick deposits make it more challenging for subsequent fuel droplets to vaporize, leading to more unburned fuels turning into deposits. Additionally, biodiesel is more prone to auto-oxidation compared to petroleum diesel, which contributes to the formation of thicker deposits [56]. Other than that, within various regions of the combustion chamber, the thickness of the deposits varied significantly. Typically, thicker deposits formed on surfaces with lower temperatures [39]. Although DF droplets impinged on a cooler surface, DF produced fewer deposits compared to the other blended fuels, indicating that the blend ratio has a more substantial impact on deposition than the effect of surface temperature.

Table 3
 Photograph of deposit at $N_D=4000$, $N_D=8000$, and $N_D=16000$ for wet condition

Fuel	Condition	Droplet number, N_D		
		$N_D=4000$	$N_D=8000$	$N_D=16000$
DF	$t_{imp}=7s$ $T_s=315^\circ C$	 0.6mg	 1.9mg	 4.4mg
		 0.5mg	 2.9mg	 8.9mg

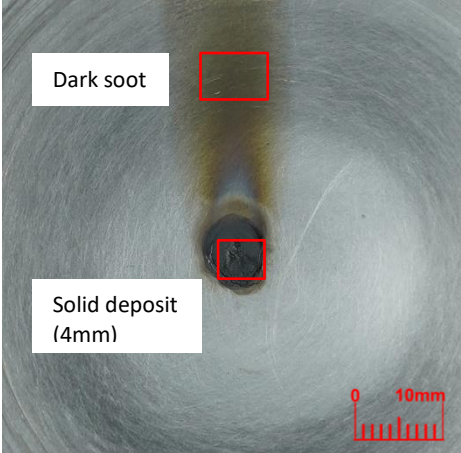
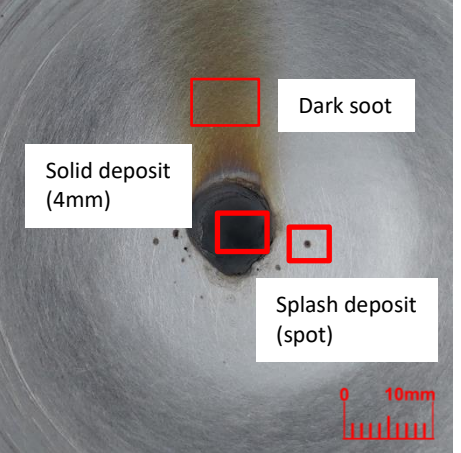
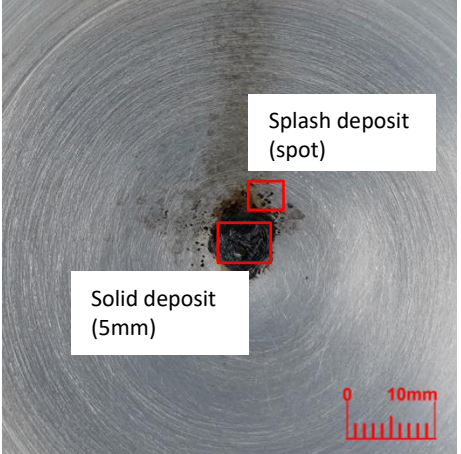
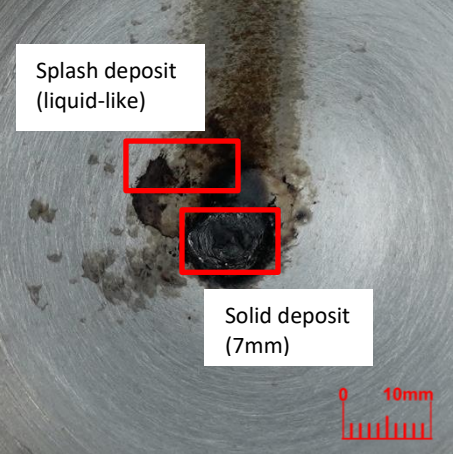
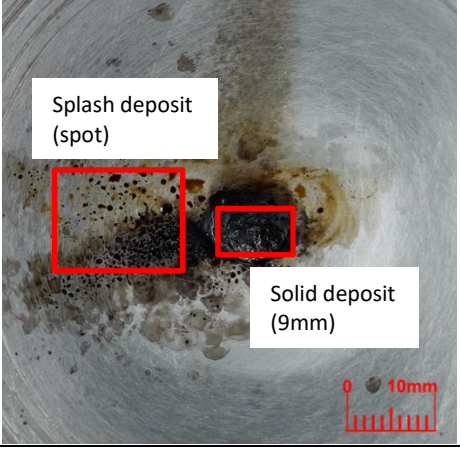
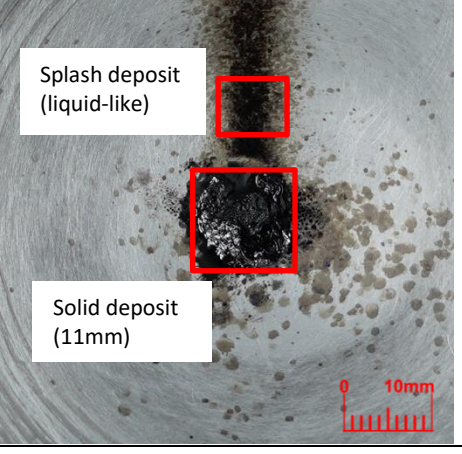


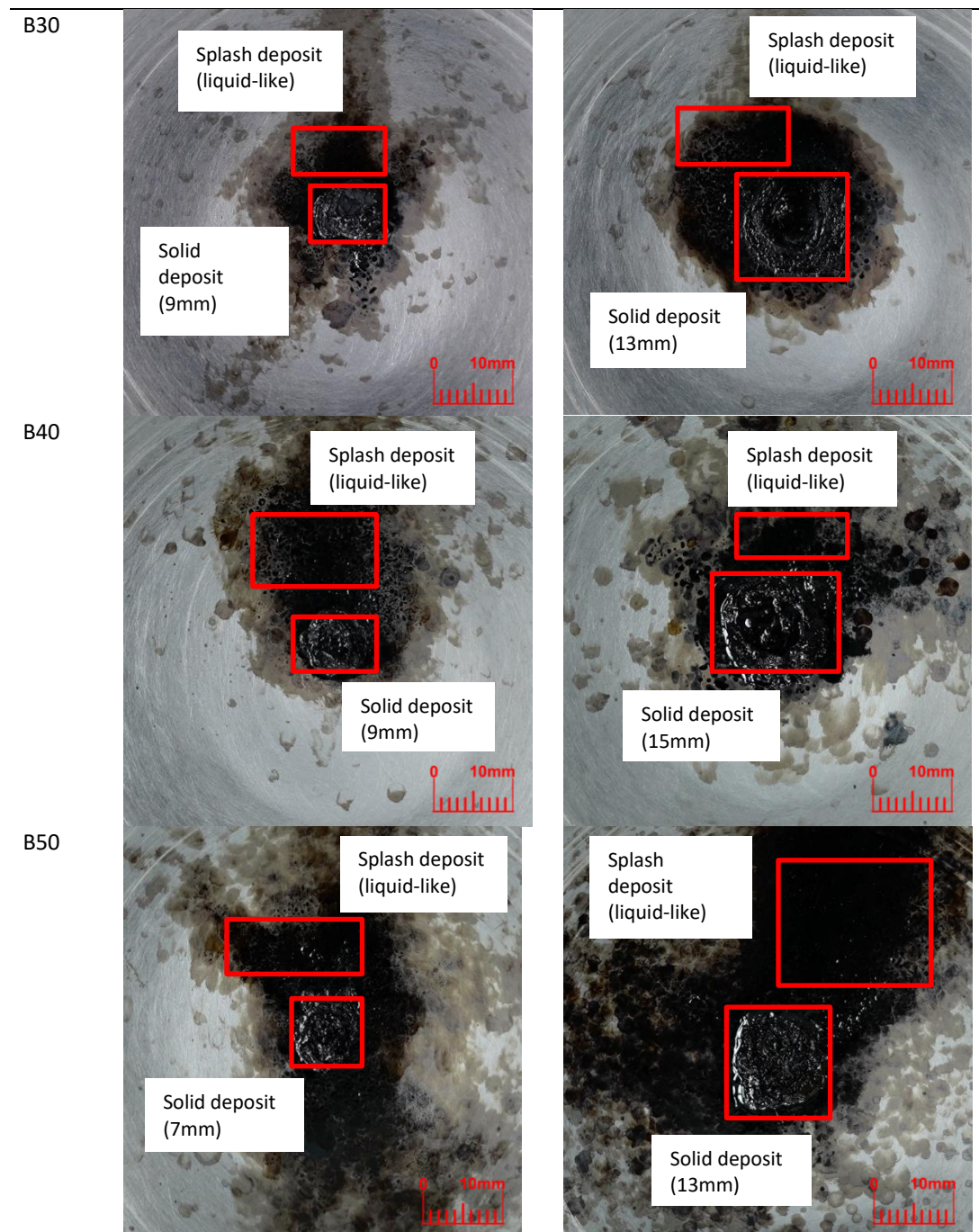
After conducting deposition tests at $N_D=16000$ under both dry and wet conditions, the solid deposit size can be determined as outlined in Table 4. When using DF, solid deposits of approximately 4mm in diameter were observed for both dry and wet conditions at $N_D=16000$. In the wet condition test, there were also a few instances of deposit splashes and dark soot accumulated on the plate due to smoke drawn in by the HSDT machine's exhaust fan. Despite leaving stains on the plate's surface, this soot did not disrupt droplet impingement or deposit formation. In the case of B10 fuel, a few deposit splashes were observed during the dry condition test, but during the wet condition test, liquid-like deposit splashes were produced. Regarding the solid deposits on the hot plate, they measured approximately 5mm in diameter for the dry condition test and 7mm for the wet condition test.

More deposit splashes were visible for B20 fuel during the dry condition test, resulting in solid deposits with an approximate diameter of 9mm. In the wet condition test, the solid deposit's diameter increased to around 11mm, and liquid-like deposit splashes were also observed on the heated plate's surface. B30 fuel showed liquid-like deposit splashes during both dry and wet condition tests, with solid deposits measuring approximately 9mm in diameter for the dry condition

and 13mm for the wet condition. For B40 and B50 fuels, liquid-like deposit splashes were evident in both dry and wet conditions. The approximate solid deposit diameters were 9mm (dry condition) and 15mm (wet condition) for B40 fuel, and 7mm (dry condition) and 13mm (wet condition) for B50 fuel.

Table 4
 Approximate diameter of the solid deposit formed at $N_D=16000$

Fuel	Condition	
	Dry	Wet
DF	 <p>Dark soot</p> <p>Solid deposit (4mm)</p>	 <p>Solid deposit (4mm)</p> <p>Splash deposit (spot)</p> <p>Dark soot</p>
B10	 <p>Splash deposit (spot)</p> <p>Solid deposit (5mm)</p>	 <p>Splash deposit (liquid-like)</p> <p>Solid deposit (7mm)</p>
B20	 <p>Splash deposit (spot)</p> <p>Solid deposit (9mm)</p>	 <p>Splash deposit (liquid-like)</p> <p>Solid deposit (11mm)</p>



Based on the data from Table 2 to Table 4, the graph of mass and solid deposit radius generated at $N_D=16000$ for both dry and wet condition tests was plotted as can be seen in Figure 2. In the figure, the radius of the solid deposit and mass of the deposit produced was greater for fuel with higher biodiesel content. Furthermore, the solid deposit radius was greater during impingement interval $t_{imp}=3$ seconds compared to $t_{imp}=7$ seconds. Significant differences in solid deposit radius produced for both test intervals were observed for B40 and B50 fuel. However, B40 fuel surpassed B50 fuel in terms of the mass of deposit produced for both test conditions. Additionally, for the wet condition test, the solid deposit radius for B50 fuel was less than that of B40. This condition aligns with data from Table 3 where at droplet $N_D=16000$, the surface of the plate during the deposition test for B40 fuel appeared to be dirtier compared to B50 fuel.

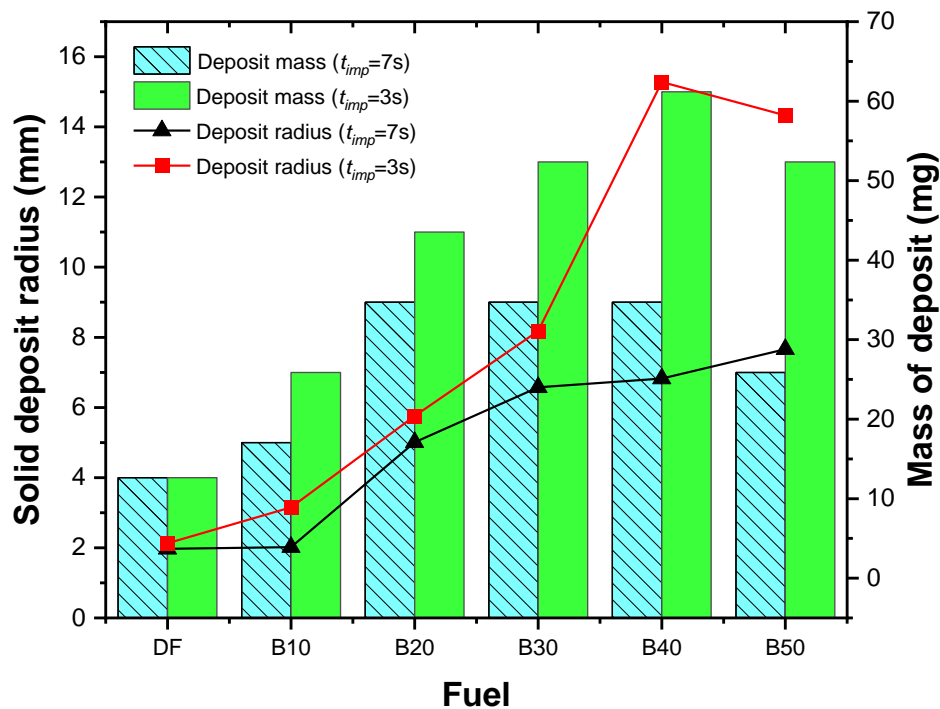


Fig. 2. Mass of deposit and solid deposit radius produced at droplet $N_D=16000$

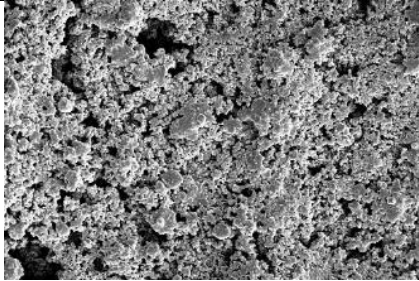
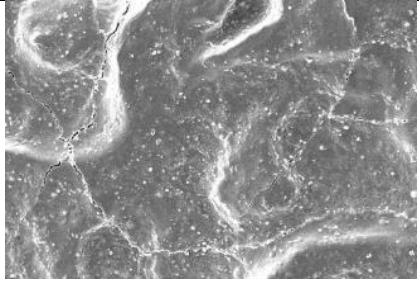
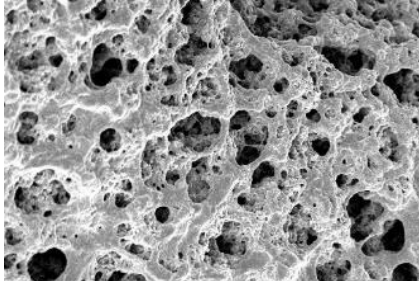
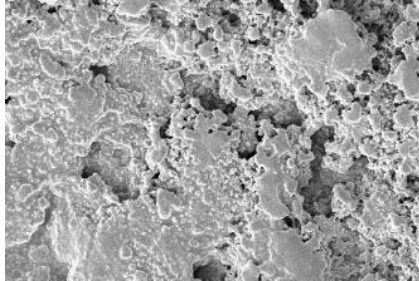
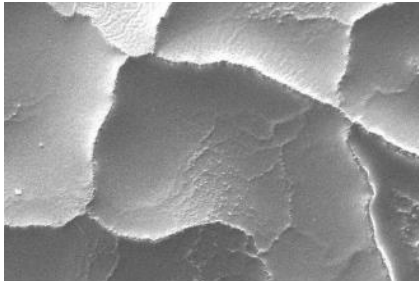
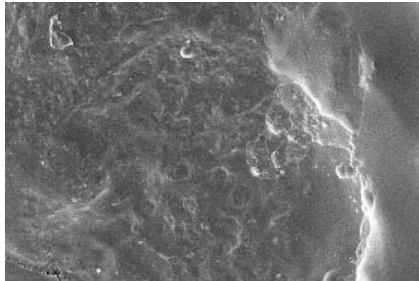
The magnified SEM images which were taken at the center region at 500x magnification of the generated deposits after droplet $N_D=16000$ were presented in Table 5. For DF, the concentration of carbon (C) and oxygen (O) were 72.89% and 27.11% for the wet condition test while 71.18% and 24.10% for C and O content during the dry condition test, respectively. The appearance of other elements could not be clarified which was silicone (Si) was detected for DF during the dry condition test. This was probably caused by contamination or the coating material that was applied onto the deposit's surface before the sample was tested in the SEM chamber. According to Liaquat *et al.*, [38], the detection of other foreign elements is possible as other factors such as contaminated lubricant could alter the deposit composition measurement. Furthermore, the magnified image of the deposit for the wet condition test for DF shows that a lot of uneven rough pores were formed. When DF is utilized, deposits do not always form with a uniform layer of carbon [54]. On the other hand, a smoother deposit surface with cracks formation appeared for the dry condition test of DF.


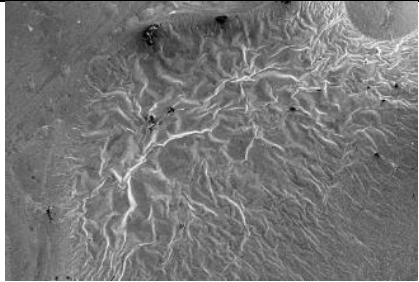
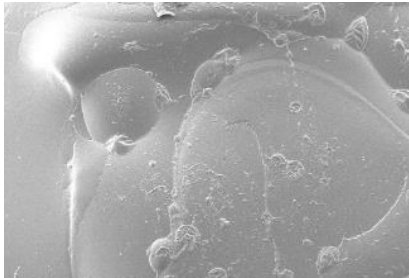
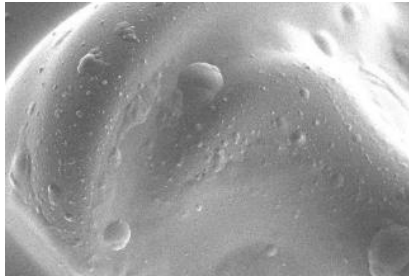
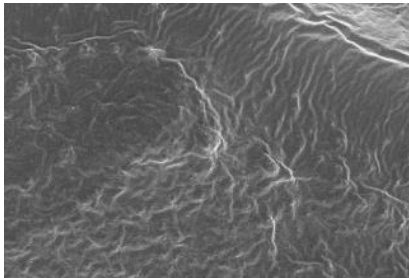
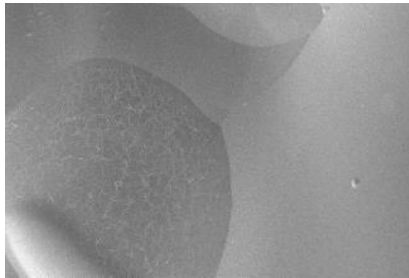
For the B10 deposit's composition, the concentration of C and O were 77.49% and 22.51% for the wet condition test. Meanwhile, for the dry condition test the composition consists of 78.68% C and 21.32% O. Larger pores were formed during the wet condition test while for the dry condition test, multiple layers of deposit were formed. These deposits' physical composition implied that the produced deposits at droplet $N_D=16000$ for both test conditions were porous and rougher.

During the wet condition test for B20 fuel, relatively higher C concentrations of 80.93% and only 19.07% of O were detected in the deposits' composition. The magnified image also shows that there were cracks formed on the deposit's surface. Surprisingly, 100% of C content was detected for the dry condition test with the absence of other elements, especially O element. For B30 fuel, the deposit's composition consists of 71.62% C and 28.38% O in the wet condition test. Furthermore, the SEM image shows a bubble-like shape appearing on the surface of the deposit. In the dry condition test, the SEM image shows a wrinkle-like surface of the formed deposit. The C concentration was lower (65.56%) while the O concentration was higher (34.44%) compared to that of the wet condition test.

For B40 fuel, a bubble-like shape was formed on the surface of the accumulated deposits for both test conditions. Moreover, no visible pores were formed and the surface of the deposit appeared to be smoother. There was also no O element detected during the wet condition test, which left the C element with 100% concentration. For the dry condition test, 67.78% of the C element and 32.22% O element were detected on the surface of the deposits. The deposits formed by B50 fuel during the wet condition test possess identical wrinkle-like surfaces as produced by that of the B30 deposit. However, the B50 deposit's composition during the wet condition test has a higher C percentage (72.64%) and a relatively lower O percentage (27.36%) compared to that of the B30 deposit during the dry condition test. In addition, there was only a C element that was detected on the surface of the deposit during the dry condition test for B50 fuel. These findings were identical to those of Liaquat *et al.*, [54] who also found out the resultant deposits of B50 contained less oxygen element in the deposit's composition despite B50 fuel containing more oxygen. The generated SEM image also shows a smooth deposit's surface with no apparent pores or cracks appearing.

Table 5
 SEM image and deposit composition mass percentage at droplet $N_D=16000$ for dry and wet condition test

Fuel	Deposit composition by weight % (Carbon (C), Oxygen (O), Others)	
	Wet ($t_{imp}=3$ seconds)	Dry ($t_{imp}=7$ seconds)
DF	 C: 72.89 O: 27.11 Others: N/A	 C: 71.18 O: 24.10 Others: Si: 4.72
B10	 C: 77.49 O: 22.51 Others: N/A	 C: 78.68 O: 21.32 Others: N/A
B20	 C: 80.93 O: 19.07 Others: N/A	 C: 100.00 O: N/A Others: N/A

B30		
	C: 71.62 O: 28.38 Others: N/A	C: 65.56 O: 34.44 Others: N/A
B40		
	C: 100.00 O: N/A Others: N/A	C: 67.78 O: 32.22 Others: N/A
B50		
	C: 72.64 O: 27.36 Others: N/A	C: 100.00 O: N/A Others: N/A

4. Conclusions

Neat diesel and biodiesel-diesel blends up to 50% by step of 10 and their deposits formation on the heated aluminum plate was studied. Based on the experimental results, the following conclusions can be drawn

- i. Visual inspection revealed that DF had accumulated some deposits. However, based on the deposition on the hot plate, it was discovered that the blended fuels (B10-B50) were dirtier.
- ii. Fuel with a higher blend ratio produced more deposits in terms of mass except for B40 fuel which exceeded the mass of the B50 deposit during the wet condition test. This indicated that the wet condition escalated the deposit accumulation rather than the blend ratio itself.
- iii. Deposits produced by DF, B10, and B20 were observed to be dry, whereas for B30, B40, and B50 the deposits produced were observed to be oily and greasy for both test conditions.
- iv. It was observed that deposit splashes were generated during the deposition test. The visibility of these deposit splashes became more pronounced as the blend ratio

- increased. Additionally, it was noted that the distribution area of deposits was broader when the test was conducted under wet conditions.
- v. The extensive area of deposit splashing indicated the gradual presence of wet conditions as the number of droplet repetitions increased. As the deposited layers became thicker, the evaporation lifetime of each subsequent fuel droplet extended, contributing to the persistence of wet conditions, especially for B20-B50 fuels.
 - vi. SEM analysis shows that the deposits' composition primarily consisted of carbon, with a relatively lower oxygen concentration. Furthermore, rough pores were formed on the surface of deposits produced by the DF and B10. SEM images also showed that the surface of deposits produced was smoother for B20, B30, B40, and B50 fuel with no visible pores.
 - vii. Despite using the same fuel, different shapes based on the deposits' morphology were observed. These were influenced by the impingement interval of the fuel droplets (dry and wet conditions).

Acknowledgement

The study is funding by Ministry of Higher Education (MOHE) of Malaysia through the Fundamental Research Grant Scheme (FRGS), No: FRGS/1/2020/TK0/UTEM/02/20. The authors also would like to thank Universiti Teknikal Malaysia Melaka (UTeM) for all the supports.

References

- [1] Rahman, Nik Kechik Mujahidah Nik Abdul, Syamimi Saadon, and Mohd Hasrizam Che Man. "Waste Heat Recovery of Biomass Based Industrial Boilers by Using Stirling Engine." *Journal of Advanced Research in Fluid Mechanics and Thermal Sciences* 89, no. 1 (2022): 1-12. <https://doi.org/10.37934/arfmts.89.1.112>
- [2] Jikol, F., M. Z. Akop, Y. M. Arifin, M. A. Salim, and S. G. Herawan. "Biofuel Development in Malaysia: Challenges and Future Prospects of Palm Oil Biofuel." *International Journal of Nanoelectronics & Materials* 15 (2022): 159-181.
- [3] Yusoff, Mohd Nur Ashraf Mohd, Nurin Wahidah Mohd Zulkifli, Nazatul Liana Sukiman, Ong Hwai Chyuan, Masjuki Haji Hassan, Muhammad Harith Hasnul, Muhammad Syahir Amzar Zulkifli, Muhammad Mujtaba Abbas, and Muhammad Zulfattah Zakaria. "Sustainability of palm biodiesel in transportation: a review on biofuel standard, policy and international collaboration between Malaysia and Colombia." *Bioenergy Research* 14, no. 1 (2021): 43-60.
- [4] Afzal, Asif, Manzoore Elahi M. Soudagar, Ali Belhocine, Mohammed Kareemullah, Nazia Hossain, Saad Alshahrani, Ahamed Saleel C, Ram Subbiah, Fazil Qureshi, and Muhammad Abbas Mujtaba. "Thermal performance of compression ignition engine using high content biodiesels: a comparative study with diesel fuel." *Sustainability* 13, no. 14 (2021): 7688. <https://doi.org/10.3390/su13147688>
- [5] Syahmi, Anwar, Mas Fawzi, Shahrul Azmir Osman, and Harrison Lau. "Engine Performance and Exhaust Emission Effect of Increasing Euro5 Diesel Fuel Blended with 7% to 30% Palm Biodiesel." *Journal of Advanced Research in Applied Sciences and Engineering Technology* 28, no. 2 (2022): 34-40. <https://doi.org/10.37934/araset.28.2.3440>
- [6] Maksom, Mohammad Syahadan, Nurul Fitriah Nasir, Norzelawati Asmuin, Muhammad Faqhrurrazi Abd Rahman, and Riyadhthusollehan Khairulfuaad. "Biodiesel composition effects on density and viscosity of diesel-biodiesel blend: a CFD study." *CFD Letters* 12, no. 4 (2020): 100-109. <https://doi.org/10.37934/cfdl.12.4.100109>
- [7] Sarwani, Muhamad Khairul Ilman, Mas Fawzi, Shahrul Azmir Osman, and Wira Jazair Yahya. "Calculation of Specific Exhaust Emissions of Compression Ignition Engine Fueled by Palm Biodiesel Blend." *Journal of Advanced Research in Applied Sciences and Engineering Technology* 27, no. 1 (2022): 92-96. <https://doi.org/10.37934/araset.27.1.9296>
- [8] Zulkurnai, Fatin Farhanah, Norhidayah Mat Taib, Wan Mohd Faizal Wan Mahmood, and Mohd Radzi Abu Mansor. "Combustion characteristics of diesel and ethanol fuel in reactivity controlled compression ignition engine." *Journal of Advanced Research in Numerical Heat Transfer* 2, no. 1 (2020): 1-13.
- [9] Mourad, M., Khaled RM Mahmoud, and El-Sadek H. NourEldeen. "Improving diesel engine performance and emissions characteristics fuelled with biodiesel." *Fuel* 302 (2021): 121097. <https://doi.org/10.1016/j.fuel.2021.121097>
- [10] Thangamani, Saravanakumar, Sathya Narayanan Sundaresan, Viraj Tatyasaheb Barawkar, and Thangaraja Jeyaseelan. "Impact of biodiesel and diesel blends on the fuel filter: A combined experimental and simulation

- study." *Energy* 227 (2021): 120526. <https://doi.org/10.1016/j.energy.2021.120526>
- [11] Fayad, Mohammed A., Miqdam T. Chaichan, and Hayder A. Dhahad. "Engine performance and PM concentrations from the combustion of Iraqi sunflower oil biodiesel under variable diesel engine operating conditions." In *Journal of Physics: Conference Series*, vol. 1973, no. 1, p. 012051. IOP Publishing, 2021. <https://doi.org/10.1088/1742-6596/1973/1/012051>
- [12] Shehata, Mohamed Saied. "Emissions, performance and cylinder pressure of diesel engine fuelled by biodiesel fuel." *Fuel* 112 (2013): 513-522. <https://doi.org/10.1016/j.fuel.2013.02.056>
- [13] Jikol, F., M. Z. Akop, Y. M. Arifin, M. A. Salim, and S. G. Herawan. "Deposits Formation, Emissions, and Mechanical Performance of Diesel Engine Fuelled with Biodiesel: A Review." *International Journal of Nanoelectronics & Materials* 15 (2022): 125-145.
- [14] Uyumaz, Ahmet, Bilal Aydoğan, Emre Yılmaz, Hamit Solmaz, Fatih Aksoy, İbrahim Mutlu, Duygu İpci, and Alper Calam. "Experimental investigation on the combustion, performance and exhaust emission characteristics of poppy oil biodiesel-diesel dual fuel combustion in a CI engine." *Fuel* 280 (2020): 118588. <https://doi.org/10.1016/j.fuel.2020.118588>
- [15] Hidayat, J. A., and Bambang Sugiarto. "Characteristic, structure, and morphology of carbon deposit from biodiesel blend." *Evergreen* 7, no. 4 (2020): 609-614. <https://doi.org/10.5109/4150514>
- [16] Sase, Akash, P. M. Ardhapurkar, and Supriya N. Bobade. "Biodiesel from thumba oil characterization and performance testing in internal combustion engine." *International Research Journal of Engineering and Technology* 3, no. 12 (2016): 511-517.
- [17] Cahyo, Nur, Ruly Bayu Sitanggang, Arionmaro Asi Simareme, and P. Paryanto. "Impact of crude palm oil on engine performance, emission product, deposit formation, and lubricating oil degradation of low-speed diesel engine: An experimental study." *Results in Engineering* 18 (2023): 101156. <https://doi.org/10.1016/j.rineng.2023.101156>
- [18] Xue, Jinlin, Tony E. Griff, and Alan C. Hansen. "Effect of biodiesel on engine performances and emissions." *Renewable and Sustainable Energy Reviews* 15, no. 2 (2011): 1098-1116. <https://doi.org/10.1016/j.rser.2010.11.016>
- [19] Urzędowska, Wiesława, and Zbigniew Stępień. "Prediction of threats caused by high FAME diesel fuel blend stability for engine injector operation." *Fuel Processing Technology* 142 (2016): 403-410. <https://doi.org/10.1016/j.fuproc.2015.11.001>
- [20] Zhang, Xusheng, Guanyun Peng, Guohao Du, Xiucheng Sun, Guohe Jiang, Xiangming Zeng, Pengfei Sun et al. "Investigating the microstructures of piston carbon deposits in a large-scale marine diesel engine using synchrotron X-ray microtomography." *Fuel* 142 (2015): 173-179. <https://doi.org/10.1016/j.fuel.2014.11.005>
- [21] Cheng, Shi-wai Steve. *A Micrographic Study of Deposit Formation Processes in a Combustion Chamber*. No. 962008. SAE Technical Paper, 1996. <https://doi.org/10.4271/962008>
- [22] Nikolakopoulos, Pantelis G. "Simulation of deposits effect on cylinder liner and influence on new and worn compression ring of a turbocharged DI engine." *Simulation Modelling Practice and Theory* 106 (2021): 102195. <https://doi.org/10.1016/j.simpat.2020.102195>
- [23] Husnawan, M., H. H. Masjuki, T. M. I. Mahlia, and M. G. Saifullah. "Thermal analysis of cylinder head carbon deposits from single cylinder diesel engine fueled by palm oil-diesel fuel emulsions." *Applied Energy* 86, no. 10 (2009): 2107-2113. <https://doi.org/10.1016/j.apenergy.2008.12.031>
- [24] Rounthwaite, Nicholas J., Rod Williams, Catriona McGiverny, Jun Jiang, Finn Giulliani, and Ben Britton. "A chemical and morphological study of diesel injector nozzle deposits-insights into their formation and growth mechanisms." *SAE International Journal of Fuels and Lubricants* 10, no. 1 (2017): 106-114. <https://doi.org/10.4271/2017-01-0798>
- [25] Cavalheiro, Leandro Fontoura, Marcelo Yukio Misutsu, Rafael Cardoso Rial, Luíz Henrique Viana, and Lincoln Carlos Silva Oliveira. "Characterization of residues and evaluation of the physico chemical properties of soybean biodiesel and biodiesel: Diesel blends in different storage conditions." *Renewable Energy* 151 (2020): 454-462. <https://doi.org/10.1016/j.renene.2019.11.039>
- [26] Elsanusi, Osama Ahmed, Murari Mohon Roy, and Manpreet Singh Sidhu. "Experimental investigation on a diesel engine fueled by diesel-biodiesel blends and their emulsions at various engine operating conditions." *Applied Energy* 203 (2017): 582-593. <https://doi.org/10.1016/j.apenergy.2017.06.052>
- [27] Pham, Van Viet. "Research and design an experimental model for the determination of deposits formation mechanism in the combustion chamber." *International Journal on Advanced Science, Engineering and Information Technology* 9, no. 2 (2019): 656-663. <https://doi.org/10.18517/ijaseit.9.2.8361>
- [28] Feld, Herbert, and Nadine Oberender. "Characterization of damaging biodiesel deposits and biodiesel samples by infrared spectroscopy (ATR-FTIR) and mass spectrometry (TOF-SIMS)." *SAE International Journal of Fuels and Lubricants* 9, no. 3 (2016): 717-724. <https://doi.org/10.4271/2016-01-9078>
- [29] Bhikuning, Annisa, Eriko Matsumura, and Jiro Senda. "A review: non-evaporating spray characteristics of biodiesel Jatropa and palm oil and its blends." *International Review of Mechanical Engineering* 12, no. 4 (2018): 364-370.

- <https://doi.org/10.15866/ireme.v12i4.14037>
- [30] Wang, Jigang, Xiaoyu Huang, Xinqi Qiao, Dehao Ju, and Chunhua Sun. "Experimental study on evaporation characteristics of single and multiple fuel droplets." *Journal of the Energy Institute* 93, no. 4 (2020): 1473-1480. <https://doi.org/10.1016/j.joei.2020.01.009>
- [31] Hoang, Anh Tuan, and Anh Tuan Le. "A core correlation of spray characteristics, deposit formation, and combustion of a high-speed diesel engine fueled with Jatropha oil and diesel fuel." *Fuel* 244 (2019): 159-175. <https://doi.org/10.1016/j.fuel.2019.02.009>
- [32] Rahman, S. M. A., I. M. R. Fattah, S. Maitra, and T. M. I. Mahlia. "A ranking scheme for biodiesel underpinned by critical physicochemical properties." *Energy Conversion and Management* 229 (2021): 113742. <https://doi.org/10.1016/j.enconman.2020.113742>
- [33] Ali, Obed M., Rizalman Mamat, Nik R. Abdullah, and Abdul Adam Abdullah. "Analysis of blended fuel properties and engine performance with palm biodiesel-diesel blended fuel." *Renewable Energy* 86 (2016): 59-67. <https://doi.org/10.1016/j.renene.2015.07.103>
- [34] Lacey, Joshua, Karthik Kameshwaran, Zoran Filipi, Peter Fuentes-Afflick, and William Cannella. "The effect of fuel composition and additive packages on deposit properties and homogeneous charge compression ignition combustion." *International Journal of Engine Research* 21, no. 9 (2020): 1631-1646. <https://doi.org/10.1177/1468087419828624>
- [35] Hasannuddin, A. K., W. J. Yahya, S. Sarah, A. M. Ithnin, S. Syahrullail, D. A. Sugeng, I. F. A. Razak et al. "Performance, emissions and carbon deposit characteristics of diesel engine operating on emulsion fuel." *Energy* 142 (2018): 496-506. <https://doi.org/10.1016/j.energy.2017.10.044>
- [36] Dhar, Atul, and Avinash Kumar Agarwal. "Effect of Karanja biodiesel blend on engine wear in a diesel engine." *Fuel* 134 (2014): 81-89. <https://doi.org/10.1016/j.fuel.2014.05.039>
- [37] Birgel, A., N. Ladommatos, P. Aleiferis, S. Zülch, N. Milovanovic, V. Lafon, A. Orlovic, P. Lacey, and Paul Richards. "Deposit formation in the holes of diesel injector nozzles: A critical review." *SAE Technical Paper 2008-01-2383* (2008). <https://doi.org/10.4271/2008-01-2383>
- [38] Liaquat, A. M., H. H. Masjuki, M. A. Kalam, M. A. Fazal, Abdul Faheem Khan, H. Fayaz, and M. Varman. "Impact of palm biodiesel blend on injector deposit formation." *Applied Energy* 111 (2013): 882-893. <https://doi.org/10.1016/j.apenergy.2013.06.036>
- [39] Kalghatgi, Gautam T. *Combustion Chamber Deposits and Knock in a Spark Ignition Engine-Some Additive and Fuel Effects*. No. 962009. SAE Technical Paper, 1996. <https://doi.org/10.4271/962009>
- [40] Zerda, T. W., X. Yuan, and S. M. Moore. "Effects of fuel additives on the microstructure of combustion engine deposits." *Carbon* 39, no. 10 (2001): 1589-1597. [https://doi.org/10.1016/S0008-6223\(00\)00287-6](https://doi.org/10.1016/S0008-6223(00)00287-6)
- [41] Zerda, T. W., X. Yuan, S. M. Moore, and CA Leon y Leon. "Surface area, pore size distribution and microstructure of combustion engine deposits." *Carbon* 37, no. 12 (1999). [https://doi.org/10.1016/S0008-6223\(99\)00068-8](https://doi.org/10.1016/S0008-6223(99)00068-8)
- [42] Barker, J., P. Richard, C. Snape, and W. Meredith. "Diesel injector deposits-an issue that has evolved with engine technology." *SAE Technical Paper 2011-01-1923* (2011). <https://doi.org/10.4271/2011-01-1923>
- [43] Kalghatgi, Gautam T. *Combustion chamber deposits in spark-ignition engines: a literature review*. No. 952443. SAE Technical Paper, 1995. <https://doi.org/10.4271/952443>
- [44] Singer, Patrick, and Jürgen Rühle. "On the mechanism of deposit formation during thermal oxidation of mineral diesel and diesel/biodiesel blends under accelerated conditions." *Fuel* 133 (2014): 245-252. <https://doi.org/10.1016/j.fuel.2014.04.041>
- [45] Suryantoro, M. T., H. Setiapraja, S. Yubaidah, Bambang Sugiarto, A. B. Mulyono, M. I. Attharik, T. Halomoan, and M. R. Ariestiawan. "Effect of temperature to diesel (B0) and biodiesel (B100) fuel deposits forming." In *AIP Conference Proceedings*, vol. 2062, no. 1. AIP Publishing, 2019. <https://doi.org/10.1063/1.5086591>
- [46] Arifin, Y. Mohamed, Y. Tsuruta, T. Furuhashi, M. Saito, and M. Arai. "Influence factors of deposits formation on a hot surface for diesel and bio-blended diesel fuel." In *The Seventh International Conference on Modeling and Diagnostics for Advanced Engine Systems (COMODIA 2008)*, pp. 799-805. 2008. <https://doi.org/10.1299/jmsesdm.2008.7.799>
- [47] Zare, Mehdi, Barat Ghobadian, Seyed Reza Hassan-Beygi, and Gholamhasan Najafi. "Evaporation Characteristics of Diesel and Biodiesel Fuel Droplets on Hot Surfaces." *Journal of Renewable Energy and Environment* 7, no. 2 (2020): 1-7.
- [48] Pham, Van Viet. "Analyzing the effect of heated wall surface temperatures combustion chamber deposit formation." *Journal of Mechanical Engineering Research & Developments (JMERE)* 41, no. 4 (2018): 17-21. <https://doi.org/10.26480/jmerd.04.2018.17.21>
- [49] Jikol, F., M. Z. Akop, Y. M. Arifin, M. A. Salim, and S. G. Herawan. "A study of steady-state thermal distribution on circular plate using ANSYS." *International Journal of Nanoelectrics and Materials* 14 (2021): 479-488.
- [50] Jikol, F., M. Z. Akop, Y. M. Arifin, M. A. Salim, and S. G. Herawan. "Transient Thermal Analysis on Convection Process

- of Circular Plate Used in Hot Surface Deposition Test Rig." *International Journal of Nanoelectronics & Materials* 15 (2022): 147-157.
- [51] Mulyono, Ary Budi, Bambang Sugiarto, Muchammad Taufiq Suryantoro, Hari Setiapraja, Siti Yubaidah, Mochammad Ilham Attharik, Muhamad Raihan Ariestiawan, and Andro Cohen. "Effect of hydrotreating in biodiesel on the growth of deposits in the combustion chamber as a solution for the deposits reduction in the usage of biodiesel." In *E3S Web of Conferences*, vol. 67, p. 02014. EDP Sciences, 2018. <https://doi.org/10.1051/e3sconf/20186702014>
- [52] Arifin, Yusmady Mohamed, Tomohiko Furuhashi, Masahiro Saito, and Masataka Arai. "Diesel and bio-diesel fuel deposits on a hot surface." *Fuel* 87, no. 8-9 (2008): 1601-1609. <https://doi.org/10.1016/j.fuel.2007.07.030>
- [53] Kalam, MdAbul, and H. H. Masjuki. "Emissions and deposit characteristics of a small diesel engine when operated on preheated crude palm oil." *Biomass and Bioenergy* 27, no. 3 (2004): 289-297. <https://doi.org/10.1016/j.biombioe.2004.01.009>
- [54] Liaquat, A. M., H. H. Masjuki, M. A. Kalam, and IM Rizwanul Fattah. "Impact of biodiesel blend on injector deposit formation." *Energy* 72 (2014): 813-823. <https://doi.org/10.1016/j.energy.2014.06.006>
- [55] Suryantoro, M. Taufiq, Bambang Sugiarto, and Fariz Mulyadi. "Growth and characterization of deposits in the combustion chamber of a diesel engine fueled with B50 and Indonesian biodiesel fuel (IBF)." *Biofuel Research Journal* 3, no. 4 (2016): 521-527. <https://doi.org/10.18331/BRJ2016.3.4.6>
- [56] Hamzah, Afiqah, Ghazali Omar, Mohd Zaid Akop, Mohd Hafidz Zakaria, Nur Natasha, Atikah Rosli, Durian Tunggal, and Politeknik Tuanku Syed Sirajuddin. "Deposit formation in the injector of a diesel engine fueled with higher blended palm biodiesel." *Jurnal Tribologi* 33 (2022): 97-112.